

 Open access • Posted Content • DOI:10.1101/2021.06.11.448040

Maintaining and escaping feedback control in hierarchically organised tissue: a case study of the intestinal epithelium — [Source link](#)

Fischer Mm, Hanspeter Herzel, Nils Bluethgen

Institutions: Charité, Humboldt University of Berlin

Published on: 11 Jun 2021 - bioRxiv (Cold Spring Harbor Laboratory)

Topics: Population

Related papers:

- [Proliferation versus regeneration: the good, the bad and the ugly.](#)
- [A matter of life and death: self-renewal in stem cells.](#)
- [Stem cell system in tissue regeneration in fish](#)
- [Defining a stem cell hierarchy in the intestine: markers, caveats and controversies](#)
- [Intestinal Stem Cells and Their Defining Niche](#)

Share this paper:    

View more about this paper here: <https://typeset.io/papers/maintaining-and-escaping-feedback-control-in-hierarchically-2zzcgt10wl>

Maintaining and escaping feedback control in hierarchically organised tissue: a case study of the intestinal epithelium

Matthias M. Fischer,^{1,*} Hanspeter Herzel,^{1,†} and Nils Blüthgen^{1,‡}

¹*Institute for Theoretical Biology, Charité and
Humboldt Universität zu Berlin, 10115 Berlin, Germany*

(Dated: June 11, 2021)

The intestinal epithelium is one of the fastest renewing tissues in mammals with an average turnover time of only a few days. It shows a remarkable degree of stability towards external perturbations such as physical injuries or radiation damage. Tissue renewal is driven by intestinal stem cells, and differentiated cells can de-differentiate if the stem cell niche is lost after tissue damage. However, self-renewal and regeneration require a tightly regulated balance to uphold tissue homeostasis, and failure can lead to tissue extinction or to unbounded growth and cancerous lesions. Here, we present a mathematical model of intestinal epithelium population dynamics that is based on the current mechanistic understanding of the underlying biological processes. We derive conditions for stability and thereby identify mechanisms that may lead to loss of homeostasis. A key result is the existence of specific thresholds in feedbacks after which unbounded growth occurs, and a subsequent convergence of the system to a stable ratio of stem to non-stem cells. A biologically interesting property of the model is that the number of differentiated cells at the steady-state can become invariant to changes in their apoptosis rate. Moreover, we compare alternative mechanisms for homeostasis with respect to their recovery dynamics after perturbation from steady-state. Finally, we show that de-differentiation enables the system to recover more gracefully after certain external perturbations, which however makes the system more prone to losing homeostasis.

Keywords: Cancer, Colon, Dedifferentiation, Intestinal epithelium, Regeneration, Tissue homeostasis

* matthias.fischer@charite.de

† h.herzel@biologie.hu-berlin.de

‡ **Corresponding author** – nils.bluthgen@charite.de

9

I. INTRODUCTION

10 A tissue is said to be hierarchically organised if it consists of different cell types constituting
11 a characteristic hierarchical structure. Generally, two classes of cells can be distinguished:
12 Adult stem cells have an unlimited capacity of indefinite self-renewal, but also differentiate
13 and thus directly or indirectly give rise to differentiated cells which perform the designated
14 function of the tissue [1]. Additionally in cases of tissue damage and regeneration the
15 dedifferentiation of differentiated cells back into cycling stem cells has been observed, for
16 instance in case of the intestinal epithelium [2, 3], the airway epithelium [4], and the kidney
17 epithelium [5]. In order to uphold the homoeostasis of such a tissue in the face of external
18 perturbations, a tight regulation of the stem cell compartment is required. In case of tissue
19 damage, stem cells need to increase proliferation according to tissue requirements; however
20 over-proliferation of the stem cell compartment must be avoided in order to prevent unlimited
21 growth [6]. Such a tight control seems to be maintained through specific feedback loops
22 exerted by differentiated cells onto the stem cell compartment regulating the size of the
23 latter [7]. In contrast, control of the dedifferentiation of differentiated cells seems to be
24 exerted by the stem cell compartment (see Tata *et al.* [4], and Beumer and Clevers [8]
25 as well as the references therein). Escaping one or multiple of these stability-conferring
26 control mechanisms may cause the tissue to lose homoeostasis and subsequently switch to a
27 behaviour of unbounded, malignant growth.

28

29 The intestinal epithelium and the colon epithelium are prime examples of such hierarchically
30 organised tissues. Despite its single-layered, simple epithelial structure it is able to withstand
31 continuous mechanical, chemical and biological insults due to its specific tissue architecture
32 in combination with a high rate of cellular turnover [9]: Stem cells residing at the bottom
33 of the intestinal crypts cycle continuously approximately once per day and give rise to new
34 cells. These cells then mature while migrating upwards, until they terminally differentiate
35 and become part of the villi, eventually committing apoptosis and being shed off into the
36 intestinal lumen [10]. Control of the intestinal and the colon stem cell compartment is
37 realised via differentiated epithelial cells releasing Indian Hedgehog (Ihh), which stimulates
38 mesenchymal cells to release Bone Morphogenic Proteins (BMPs). These, in turn, interfere
39 with intracellular effects of WNT signalling and thus stimulate stem cell differentiation [11–15].

40

41 Previous theoretical research on hierarchically organised tissues has often focussed on the
42 abstract case of arbitrary tissues: Rodriguez-Brenes *et al.* [16] considered arbitrary hierar-
43 chically organised tissues consisting of two compartments: a compartment of cycling and
44 differentiating stem cells, and a compartment of non-cycling differentiated cells committing
45 apoptosis at a fixed rate. They assumed that the differentiated cell compartment may exert
46 feedback onto the stem cells by both decreasing their rate of proliferation and by reducing
47 the probability of a stem cell division resulting in two daughter stem cells compared to the
48 probability of a division yielding two differentiated cells. They then studied the order in
49 which mutations in these feedbacks need to arise in a single new clone to enjoy a selective
50 advantage and spread throughout the system. Limiting their model to sigmoidal *Hill*-like
51 feedback functions, they then also fitted their model to a number of time-course data of the
52 overall population size of growing tissue from the literature. The same model was used in
53 Rodriguez-Brenes *et al.* [17] in order to reveal that during recovery from an injury significant
54 damped oscillations in the path back to the steady-state may occur, and that this oscillatory
55 behaviour is more pronounced when the stem cell load represents only a small fraction of the
56 entire cell population. Nonetheless, oscillations may still be avoided, however at the price of
57 slowing down the speed at which the system is able to recover after an injury. The same
58 model topology has also been studied by Sun and Komarova [18] using the framework of a
59 two-dimensional Markov process in order to obtain analytical solutions for the mean and
60 variance of the cell compartment sizes. Recently, Wodarz [19] has extended the model by also
61 taking into account the possibility of differentiated cells dedifferentiating into cycling stem
62 cells again. Assuming sigmoidal *Hill*-like feedback onto stem cell cycling rate and self-renewal
63 probability, he studied the effect of a linear and a sigmoidal dedifferentiation term, showing
64 how unbounded, cancerous tissue growth may arise as a consequence of escaping this feedback.
65 By means of numerical simulations, he also demonstrated how dedifferentiation may allow
66 for speedier regeneration dynamics after perturbations.

67

68 More concrete theoretical studies have for example been carried out on the hematopoietic sys-
69 tem [20–24], the mammalian olfactory epithelium [25, 26], or on the development, treatment
70 and recurrence of breast cancer [27]. In contrast, however, theoretical examinations on the
71 homoeostasis and dynamics of the intestinal and colon epithelium have been rare. A note-

72 worthy exception is Johnston *et al.* [28], who have derived and studied a three-compartment
73 ODE model consisting of stem, transit-amplifying and terminally differentiated cells. They
74 assumed that the first two of these three compartments limit themselves either via a negative
75 quadratic term (reminiscent of classical single-species population dynamic models which
76 assume logistic growth [29]) or via a negative saturating term. However, no mechanistic
77 justification of these models has been presented in the paper, possibly also owing to the fact
78 that our mechanistic understanding of the biology of intestinal stem cells has been rather
79 limited until very recently [9].

80

81 In this work, we set out to derive a model of intestinal and colon epithelial population
82 dynamics based on our current understanding of the involved underlying biological processes.
83 We use this model in order to answer some fundamental questions about maintaining and
84 losing the homeostatic stability of this system: Both for the case without dedifferentiation
85 and for the case with dedifferentiation, we derive all possible ways the system can lose
86 stability and exhibit unbounded malignant growth. We prove analytically how allowing for
87 dedifferentiation opens up an additional way of losing stability and switching to unbounded
88 growth. For all cases of unbounded growth, we prove that – under the biologically reasonable
89 assumption of saturating rate functions – after some period of transient behaviour the system
90 will always converge to a stable ratio of cell types which we can calculate analytically. A
91 special focus is given to the study of the transient behaviour of the system while recovering
92 from different kinds of external perturbations. We examine how the shape of the feedback
93 functions shapes the system behaviour during recovery, and will compare how graceful and
94 efficient the colon model is able to recover from different kinds of external perturbations
95 compared to other imaginable model topologies throughout the entire model parameter
96 space. Finally, we show analytically and illustrate with numerical simulations how adding
97 dedifferentiation can tremendously speed up recovery and reduce frequency and duration of
98 oscillations, which especially applies to the case of perturbations of the stem cell compartment.

99

II. MATERIALS AND METHODS

100

A. Colon epithelium model

101 Our main model consists of two cell compartments S and D , denoting stem cells, and
102 differentiated cells, respectively, following earlier approaches such as Rodriguez-Brenes *et al.*
103 [16]. Stem cells cycle at a constant rate $\beta > 0$, whereas differentiated cells are cell-cycle
104 arrested, but die with an apoptosis rate $\omega > 0$. Finally, stem cells differentiate with a rate
105 $\delta(D)$ that is a function of the size of the differentiated cell compartment. Overall, the model
106 is described by the following set of two coupled ordinary differential equations:

$$\begin{aligned}\frac{dS(t)}{dt} &= \beta S(t) - \delta(D)S(t) \\ \frac{dD(t)}{dt} &= \delta(D)S(t) - \omega D(t),\end{aligned}\tag{1}$$

107 where $\beta, \omega \in \mathbb{R}^+$ and δ is a continuously differentiable and monotonically increasing function
108 $\mathbb{R}^+ \rightarrow \mathbb{R}^+$. A sketch of the model is shown in Figure 1a. Note that at this model does not
109 include the possibility of dedifferentiation, and we will extend this later.

110

111 At this point, the structural similarity between our model and the classical Lotka-Volterra
112 model of predator-prey dynamics [30, 31] may also be pointed out. In particular, if δ is a
113 linear function with an intercept of zero, i.e. if the basal stem cell differentiation rate in
114 the absence of differentiated cells is zero, then the models are mathematically identical. As
115 remarked by Peschel and Mende [32], however, even such minor qualitative changes to the
116 Lotka-Volterra model will affect its qualitative behaviour and cause the loss of its typical
117 harmonic oscillations and for instance the emergence of a limit cycle or a stable steady-state
118 instead.

119

B. Comparison of different model topologies

120 Next, we generalise the previous model to the family of all models containing exactly one
121 explicit feedback loop from one compartment onto one rate parameter. Since we have
122 two compartments which could potentially be able to exert a feedback (stem cells S , and
123 differentiated cells D), and three rates which could potentially be affected by such a feedback

124 (stem cell proliferation, stem cell differentiation, and apoptosis of differentiated cells), we get
125 a family of six possible models. It may be noted that this enumeration does not include any
126 additional implicit feedback loops which may for instance arise as a consequence of enzyme
127 sequestration [33]. We will compare these six models with each other with respect to their
128 relaxation dynamics after perturbations.

129 **C. Numerical simulations**

130 Numerical simulations have been implemented in the Python programming language [34],
131 version 3.7.3. All computations have been carried out on a 64-bit personal computer with an
132 Intel Core i5-3350P quad-core processor running Manjaro Linux, kernel version 5.6.11-1.

133

134 We provide the complete commented source code of our numerical examinations in the form
135 of an iPython jupyter notebook in the following github repository: [https://github.com/](https://github.com/Matthias-M-Fischer/Epithelium)
136 [Matthias-M-Fischer/Epithelium](https://github.com/Matthias-M-Fischer/Epithelium).

137 **D. Colon epithelium model with dedifferentiation**

138 Finally, we extend the model by a dedifferentiation process of differentiated cells into stem
139 cells. We model the rate of such a dedifferentiation to be determined by the size of the stem
140 cell compartment, where a higher number of stem cells reduces dedifferentiation. Introducing
141 an differentiable and monotonically decreasing function $\varrho : \mathbb{R}^+ \rightarrow \mathbb{R}^+$ describing the rate of
142 dedifferentiation, the model reads:

$$\begin{aligned} \frac{dS(t)}{dt} &= \beta S(t) - \delta(D)S(t) + \varrho(S)D \\ \frac{dD(t)}{dt} &= \delta(D)S(t) - \varrho(S)D - \omega D(t). \end{aligned} \tag{2}$$

143 A sketch of the model is shown in Figure 4a.

144

III. RESULTS

145

A. A population dynamics model of the colon epithelium

146 We developed a model of the intestinal epithelial population dynamics (see Fig. 1a for a
147 schematic overview, and Materials and Methods). The model distinguishes between two
148 compartments: Stem cells that cycle at a rate β and differentiate at a rate $\delta(D)$, and
149 differentiated cells that commit apoptosis and leave the system at a rate ω . We model the
150 differentiation rate as a positive function of the size of the differentiated cell compartment
151 D . This reflects the results of experimental studies demonstrating that differentiated cells
152 release Indian Hedgehog (*Ihh*) that leads to an increased mesenchymal release of Bone
153 Morphogenic Protein (*BMP*), which in turn stimulates the differentiation of intestinal stem
154 cells [11, 12].

155

156

1. Stability can be lost via two routes

157 First we study the steady-states of system (1). For now, we will not use any specific function
158 δ and only demand that δ is a positive, monotonic and continuously differentiable function.
159 We also assume $d\delta/dD \geq 0$, since differentiated cells stimulate stem cell differentiation.

160

161 By solving $dS(t)/dt = dD(t)/dt = 0$ we find two steady-states: A trivial steady-state
162 ($\bar{S} = 0, \bar{D} = 0$) that exists under all parameter values. Under some conditions, also a
163 non-trivial steady-state exists at $\bar{S} = \omega\bar{D}/\beta$ and $\bar{D} = \delta^{-1}(\beta)$. Here, δ^{-1} denotes the inverse
164 function of δ . This non-trivial steady-state exists if the function δ can reach the value of β .
165 Thus, this second steady-state is only present if the maximal differentiation rate is higher
166 than the proliferation rate. It is interesting to see that the steady-state does not depend
167 on the apoptosis rate ω . This is a biologically interesting property which we will return to later.

168

169 To address the stability of the steady-states, we investigate the Jacobian [35] of the system:

$$\mathbf{J} = \begin{pmatrix} \beta - \delta(D) & -S\delta'(D) \\ \delta(D) & S\delta'(D) - \omega \end{pmatrix},$$

170 which at the trivial steady-state has the eigenvalues $\lambda_1 = \beta - \delta(0)$, $\lambda_2 = -\omega < 0$. Hence,
171 the trivial steady-state is only stable, if the proliferation rate β is smaller than the basal
172 differentiation rate $\delta(0)$.

173

174 At any non-trivial steady-state, the Jacobian is given by

$$\mathbf{J}_{s-s} = \begin{pmatrix} 0 & -S\delta'(\bar{D}) \\ \beta & S\delta'(\bar{D}) - \omega \end{pmatrix}.$$

175 The steady-state is stable if $\det \mathbf{J}_{s-s} > 0$ and $\text{tr} \mathbf{J}_{s-s} < 0$ (Routh–Hurwitz criterion, see
176 Strogatz [36]), which leads to $0 < \delta'(\bar{D}) < \delta(\bar{D})/\bar{D}$.

177

178 These results reveal two routes of how the intestinal epithelium can lose homeostasis and
179 show altered qualitative behaviour (Fig. 1b): First, the tissue might show unbounded growth,
180 which could be interpreted as the emergence of a cancerous lesion (Fig. 1b, second column).
181 This occurs once the proliferation rate β exceeds the maximum differentiation rate δ_{max}
182 (either by increased proliferation or decreased maximal differentiation). In this case, only the
183 (unstable) steady-state $(0, 0)$ remains, and any positive perturbation of S away from it will
184 lead to unbounded growth

185

186 Second, the steady-state $\bar{D} = \delta^{-1}(\beta)$ can get unstable if $\delta'(\bar{D}) < \delta(\bar{D})/\bar{D}$. In other words, at
187 the steady-state the slope of the feedback function might exceed $\delta(\bar{D})/\bar{D}$. When this happens,
188 the behaviour of the system depends on the feedback function. This can be illustrated with
189 the following two examples:

190

191 First, consider a linear function of the form $\delta(D) = \delta_0 + \delta_{slope}D$. For instability, we require
192 that $\delta'(\bar{D}) > \beta/\bar{D}$, hence the system will only be stable for a strictly positive intercept
193 δ_0 . This is biologically plausible, since the intercept denotes the basal differentiation rate
194 of stem cells in the absence of any external stimuli, which can be expected to exceed
195 zero. If, however, the intercept is zero then the fix point will not be stable. This case
196 is equivalent to the classical Lotka-Volterra model of predator-prey population dynamics,
197 exhibiting undamped oscillations. As second example, consider a sigmoid function of
198 the form $\delta(D) = \delta_0 + \delta_{max}D^p/(D_{min}^p + D^p)$. For instability, we require that $\delta'(\bar{D}) > \beta/\bar{D}$.

199 Hence, at $p > 4\beta/\delta_{max}$ the steady-state loses its stability, and the system will show sustained
200 oscillations.

201 *2. Exponential growth and convergence to a stable cell type ratio after escaping control*

202 Next, we want to analyse the behaviour of system (1) when no non-trivial steady-state
203 exists and the system shows unbounded growth. This case corresponds to a tissue that has
204 escaped homeostatic control and has degenerated into a cancerous lesion. In our model,
205 this occurs when β exceeds the maximum of δ . This implies that the feedback function δ
206 has a maximum value $\delta_{max} < \beta$. Such saturation of the differentiation rate could arise from
207 saturated signalling or thermodynamical constraints.

208

209 Interestingly, during such unbounded growth the system will always converge to a stable
210 ratio of stem cells and differentiated cells ($S(t)/D(t) = \text{const}$ for $t \rightarrow \infty$). The dynamics of
211 the system is then governed by the following differential equations:

$$\begin{aligned}\frac{dS(t)}{dt} &= (\beta - \delta_{max})S(t) \\ \frac{dD(t)}{dt} &= \delta_{max}S(t) - \omega D(t).\end{aligned}$$

212 We are able to directly solve such a linear system analytically by first solving $S(t)$, yielding
213 a simple exponential function, and subsequently solving $D(t)$. Overall, we get:

$$\begin{aligned}S(t) &= S_0 e^{(\beta - \delta_{max})t} \\ D(t) &= D_0 e^{-\omega t} + S_0 \delta_{max} e^{-\omega t} \int_{s=0}^{s=t} e^{(\beta - \delta_{max} + \omega)s} ds.\end{aligned}$$

214 Because the second term of $D(t)$ grows without bounds, we may for sufficiently big values of
215 t neglect the decaying first term of $D(t)$. Calculating the integral then yields

$$D(t) = \frac{S_0 \delta_{max}}{\beta - \delta_{max} + \omega} e^{(\beta - \delta_{max})t}.$$

216 This allows us to take the following limit

$$\lim_{t \rightarrow \infty} \frac{S(t)}{D(t)} = \frac{\beta + \omega}{\delta_{max}} - 1,$$

217 which denotes the ratio of stem to differentiated cells the system will converge to during
 218 explosive growth after some transient period.

219

220 Additionally, one may easily see that after the transient period, the overall growth of the
 221 system amounts to

$$S(t) + D(t) = S_0 \frac{\beta + \omega}{\beta + \omega - \delta_{max}} e^{(\beta - \delta_{max})t},$$

222 which implies an exponential growth at a constant rate $\beta - \delta_{max}$, which is also the dominant
 223 eigenvalue of the linear system. Figure 1c provides an exemplary numerical simulation of
 224 the system with a piecewise linear feedback function $\delta(D) = \min\{0.9 + 10^{-4}D, 1.0\}$, and
 225 parameters $\beta = 1.1$ and $\omega = 0.1$. Observe the convergence of the ratio $S(t)/D(t)$ to a stable
 226 ratio of $-1 + (\beta + \omega)/\delta_{max} \approx 0.2$, which is in agreement with our theoretical analysis.

227

3. Bifurcation analysis for the case of piecewise linear δ

228 Now, we want to further analyse the influence of system parameters on the qualitative and
 229 quantitative behaviour of system 1. To this end, we now chose a concrete differentiation
 230 rate function δ . For simplicity, we chose a piecewise linear function with a positive intercept
 231 $\delta_0 > 0$, denoting the basal differentiation rate of stem cells in the absence of any external
 232 cues. We assume that δ grows linearly in D with a slope of $\delta_{slope} > 0$, until it reaches an
 233 upper bound δ_{max} , at which point it stops increasing. Hence, we have

$$\delta(D) = \begin{cases} \delta_0 + \delta_{slope}D & \delta_0 + \delta_{slope}D \leq \delta_{max} \\ \delta_{max} & \text{else} \end{cases}, \quad (3)$$

234 where $\delta_0, \delta_{slope}, \delta_{max} > 0$.

235

236 The non-trivial steady-state resides at $\bar{S} = \omega \bar{D}/\beta, \bar{D} = (\beta - \delta_0)/\delta_{slope}$ and can only exist
 237 if $\beta < \delta_{max}$. The steady-state is only biologically feasible ($\bar{S}, \bar{D} > 0$) if $\delta_0 < \beta$. Then, the
 238 Jacobian at the steady-state is given by

$$\mathbf{J}_{eq} = \begin{pmatrix} 0 & -\frac{(\beta - \delta_0)\omega}{\beta} \\ \beta & \frac{(\beta - \delta_0)\omega}{\beta} - \omega \end{pmatrix},$$

239 which has the eigenvalues

$$\lambda_{1,2} = \frac{-\delta_0\omega \pm \sqrt{-4\beta^3\omega + 4\beta^2\delta_0\omega + \delta_0^2\omega^2}}{2\beta}.$$

240 If

$$\beta - \delta_0 < \frac{\delta_0^2\omega}{4\beta^2}$$

241 the radicand is positive. Then, due to $\delta_0 < \beta$ both eigenvalues will be negative and real,
242 hence the steady-state is a stable node. If, however, the radicand is negative, oscillations
243 occur and the real part of the eigenvalues is always negative due to $\delta_0 > 0$, making the
244 steady-state a stable focus. In any case, any biologically feasible steady-state of this system
245 will always be stable.

246

247 Biologically, it is interesting that no other constraints on δ_0 and δ_{slope} are required except
248 for, $\delta_0 < \beta$, which we require for a feasible steady-state, and $\beta < \delta_{max}$. Particularly,
249 $\delta_0 > 0, \delta_{slope} > 0$ can be arbitrarily small, yet the system remains stable. Similarly, changes
250 in $\omega \geq 0$ will not affect the stability of the system. Figure 1d illustrates these findings and
251 shows bifurcation plots of the system for varying parameters $\beta, \omega, \delta_0, \delta_{slope}$.

252

253 4. *The feedback loop can cause oscillatory behaviour in cell numbers*

254 Next, we investigated the behaviour when the system shows dampened oscillations around
255 the steady-state. For any given steady-state \bar{S}, \bar{D} it holds that $\delta_0 = \beta - \delta_{slope}\bar{D}$. This permits
256 to express the eigenvalues $\lambda_{1,2}$, and thus the amplitude decay and the angular frequency of
257 the dampened oscillations in terms of δ_{slope} instead of δ_0 . We find that the amplitude of the
258 oscillations will decay with

$$\sim e^{\frac{\delta_{slope}\bar{D}\omega - \beta\omega}{2\beta}t}.$$

259 Note that at any equilibrium the exponent is always negative because from $\bar{D} = (\beta - \delta_0)/\delta_{slope}$
260 it follows that $\delta_{slope}\bar{D} - \beta = -\delta_0 < 0$. The angular frequency of oscillations reads

$$\omega_0 = \sqrt{\delta_{slope} \bar{D}(4\beta^2\omega + \omega^2) - \beta\omega^2/2\beta}.$$

261 Hence, a higher slope of the feedback function δ will result in a slower decrease in the
262 amplitude of oscillations, as well as cycle with a higher frequency. We provide a set of
263 numerical simulations of the system with a piecewise linear function δ as defined before and
264 varying values of δ_{slope} in Panel (e) of Figure 1 in order to illustrate our finding.

265

266 The relationship between function slope and oscillatory behaviour of the system is a bio-
267 logically interesting result, as it suggests that in order to keep the occurring oscillations in
268 check, a smaller slope of the feedback function might be desirable. For very small slopes, the
269 difference between β and δ_0 needs to become sufficiently small as well, if the position of the
270 steady-state (\bar{S}, \bar{D}) should remain constant. Then, the oscillations will complete vanish, and
271 the steady-state becomes a stable node, as shown previously.

272

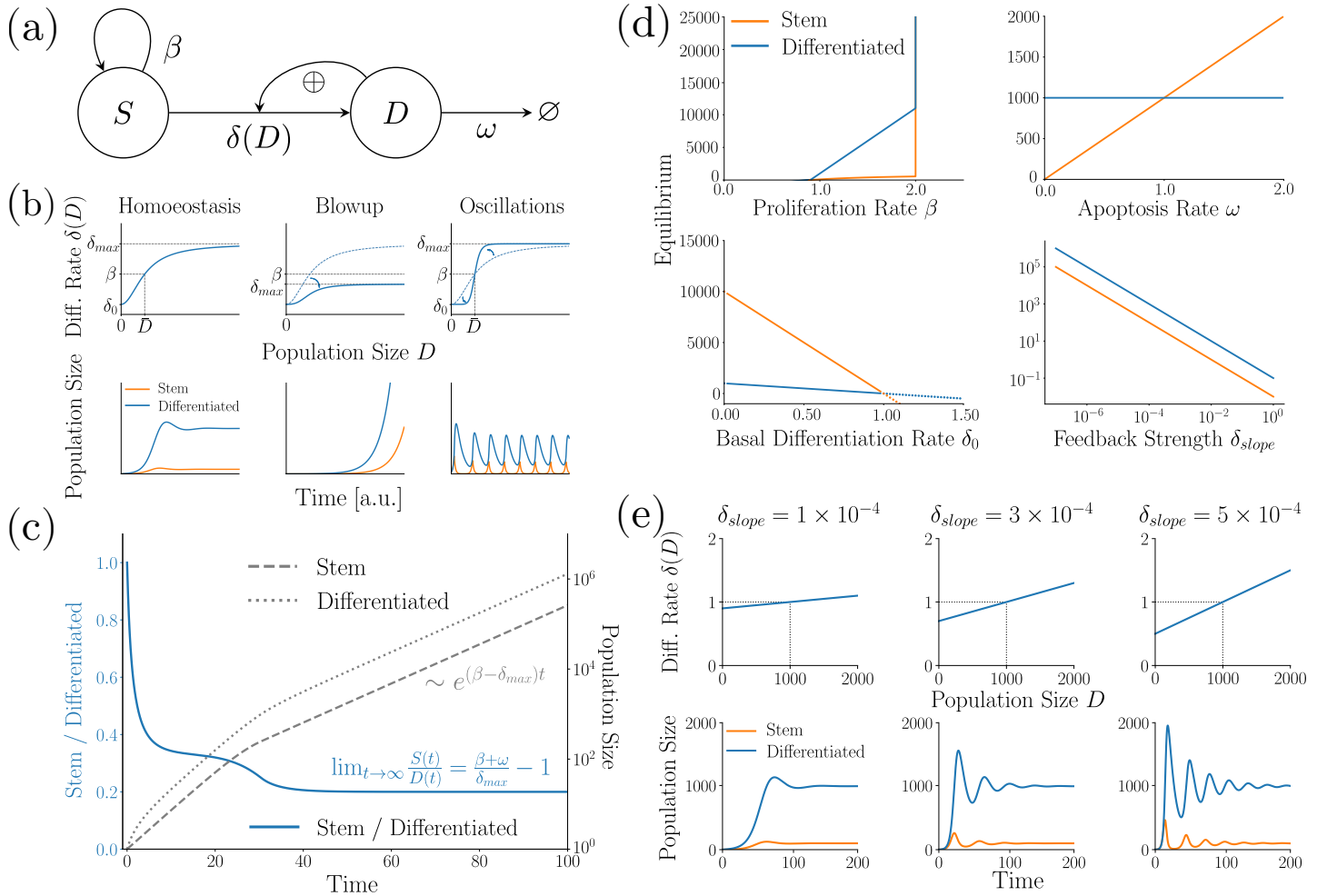
273 **B. Comparison of different model topologies**

274 In the previous section, we have shown that the colon epithelium model can cause homeostasis
275 through a feedback from differentiated cells to stem cell differentiation. In the following, we
276 explore how alternative feedback topologies in our two-compartment colon model might alter
277 tissue homeostasis, and compare the properties of these models. We therefore generated all
278 six one-looped topologies.

279

280 *1. Controlling stem cells is required for stability*

281 First, we consider those two topologies where the apoptosis rate ω is regulated by either the
282 size of the stem cell compartment S or the size of the compartment of differentiated cells
283 D , respectively. Both topologies are not able to show homeostasis: If both the stem cell
284 proliferation rate β and differentiation rate δ are unregulated and hence constant, we have
285 $dS(t)/dt = \beta S - \delta S$, which for any non-trivial steady-state requires $\beta = \delta$. This, in turn,
286 implies that $dS(t)/dt = 0$ at all points of time, hence after any perturbation of S , S will not



287 be able to return to its pre-perturbation state. Accordingly, these models are biologically

288 not realistic, and we will not consider them in the rest of this paper.

289

290 *2. Indirect regulation of the stem cell compartment decouples the steady-state number of*
291 *differentiated cells from their apoptosis rate*

292 Next, we generalise our previous finding that in the colon epithelium model the steady-state
293 \bar{D} of differentiated cells is invariant to changes in ω to other model topologies. In fact, all
294 models in which proliferation and differentiation of the stem cell compartment is exclusively
295 regulated by the size of the differentiated cell compartment D following arbitrary continuously
296 differentiable functions $\beta(D), \delta(D)$ enjoy this property: Let $dS(t)/dt = \beta(D)S - \delta(D)S$. At
297 any non-trivial steady-state (\bar{S}, \bar{D}) , from $dS(t)/dt = 0$ we get that $\beta(\bar{D}) = \delta(\bar{D})$. Define
298 $\alpha(D) := \beta(D) - \delta(D)$, then $\bar{D} = \alpha^{-1}(0)$, which does indeed not depend on our choice of
299 ω . This is biologically interesting since it is desirable from a physiological point of view to
300 keep the number of differentiated cells as constant as possible, because differentiated cells
301 are responsible for carrying out the primary function of a tissue. In contrast, $\bar{S} = \omega\bar{D}/\beta(\bar{D})$
302 depend linearly on ω . Also note that for the opposite case of a stem cell compartment which
303 is only regulated by its own size, \bar{S} is invariant to changes in ω , but \bar{D} depends linearly on it.

304

305 *3. Saturating feedback functions β and δ cause convergence to a stable cell type ratio during*
306 *unbounded growth*

307 Finally, it may also be briefly noted that all systems in which proliferation and differentiation
308 rates of the stem cell compartment are functions saturating to β_{min} and δ_{max} for sufficiently big
309 D respectively, will in case of unbounded growth converge to a stable ratio $S(t)/D(t) = \text{const}$
310 for $t \rightarrow \infty$, given as:

$$\lim_{t \rightarrow \infty} \frac{S(t)}{D(t)} = \frac{\beta_{min} + \omega}{\delta_{max}} - 1.$$

311 4. *Differences in relaxation dynamics of different model topologies after perturbations*

312 In this section, we compare the relaxation dynamics of the four remaining model topologies
313 after applying external perturbations from steady-state, again using simple piecewise linear
314 feedback functions to keep the analyses traceable. We will examine three different kinds of
315 perturbations, which are: first, removing all differentiated cells; second, removing all but one
316 stem cell; and third, both of these perturbations at the same time. Because of bilinear terms
317 in the equations, we cannot in all cases obtain exact analytical solutions of the occurring
318 dynamics, but use approximations of the dynamics based on a linearisation of the systems
319 around their respective non-trivial steady-state (see Appendix A for details).

320

321 The Jacobian matrices and their eigensystems for the remaining four models are shown
322 in Figure 2, along with schematic model sketches and exemplary numerical simulations,
323 illustrating typical solutions.

324

325 Physiologically, it is important that the number of differentiated cells recovers quickly, as these
326 are the cells responsible for carrying out the function of the respective tissue – for instance,
327 the secretory and absorptive cells of the colon epithelium are all terminally differentiated
328 cells. We hence compare the models based on their 'defect' χ of differentiated cells after
329 perturbation – see Panel (a) of Figure 3 for an illustration. We define the defect as the total
330 area between $D(t)$ after a perturbation at $t = 0$ and \bar{D} , i.e.

$$\chi := \int_{\substack{t=0 \\ D(t) < \bar{D}}}^{\infty} \bar{D} - D(t) dt$$

331 .

332 The defect integrates only those time intervals in which $D(t) < \bar{D}$, as this defines the lack in
333 functionality.

334

335 For all four models and the three types of perturbations, we derived either an analytical
336 expression for the defect, or – if these are expressions too complicated for a meaningful
337 analysis and interpretation – an approximate solution (see Appendix A). Three relations
338 simplify their analysis: First, for all models we obtain $\omega = \beta \bar{S} / \bar{D}$. Second, the slope

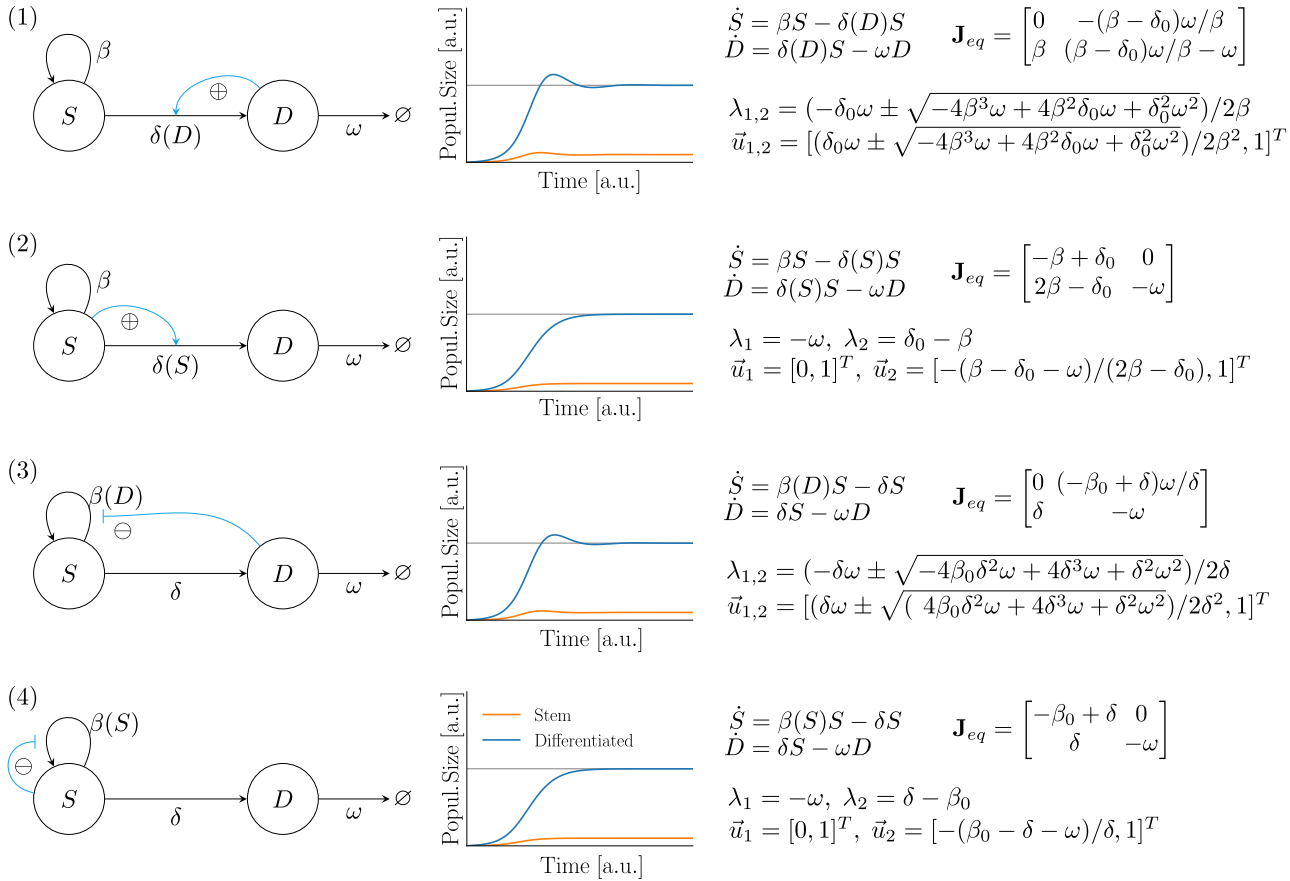


FIG. 2. All four one-looped model topologies that can show homoeostasis. First column: schematic sketches; second column: exemplary numerical simulations; third column: model equations, as well as Jacobian at the non-trivial steady-state and its eigensystem for the case of a linear feedback function $\beta(x) = \beta_0 + \beta_{slope}x$ or $\delta(x) = \delta_0 + \delta_{slope}x$, respectively.

339 of the feedback function (β_{slope} or δ_{slope} , respectively) is not required for describing the
 340 dynamics relative to the steady-state, as the slope is not part of the eigensystems of the
 341 steady-state Jacobians of the models. Third, we notice that the displacements of all models
 342 from steady-state of the first and second perturbation is linear in the initial displacement
 343 ($\Delta D(0)$ or $\Delta S(0)$, respectively). This indicates that in both cases the choice of initial
 344 displacement will not affect the comparison of the model defects, and we can express all
 345 defects as multiples of initial displacement. In case of the third perturbation, however,
 346 displacements are linear in $\Delta D(0)$, and contain an additional expression linear in $\Delta S(0)$.
 347 However, because at the steady-state the ratio of stem to differentiated cells is fixed, these
 348 two terms directly depend on each other, and we can express the defect as multiples of the

349 initial displacement of differentiated cells. Overall, this means the complete parameter space
350 we need to consider consists only of the ratio of stem to differentiated cells at steady-state
351 and two additional free parameters (depending on the model β_0, δ or β, δ_0).

352

353 *a. Colon model vs. direct stimulation of stem cell differentiation* We start by comparing
354 our basic colon epithelium model, which is model 1 in our list, with model 2, where stem cell
355 differentiation is not stimulated by the differentiated cell compartment, but instead by the
356 stem cell compartment itself (see Panel (b) of Figure 3). Panel (c) of Figure 3 shows the dif-
357 ference in model defects throughout the parameter space (see Figures 5 and 6, Appendix B for
358 the raw values), where areas shaded in red indicate region where our colon epithelium model
359 has a bigger defect than the alternative model. In case of removing differentiated cells (first
360 row) or removing both differentiated and stem cells at the same time (third row), there always
361 exist ample regions (shaded in blue) where the colon model recovers more efficiently – namely,
362 whenever the basal differentiation rate δ_0 of stem cells is close to the stem cell cycling rate
363 β . This makes sense, because in case of the colon epithelium model removing differentiated
364 cells will cause the stem cells to differentiate more slowly and thus grow in numbers quickly,
365 thus being able to replenish the differentiated cell compartment more quickly. However, in
366 case of removing only stem cells (second row), the colon epithelium model always performs
367 worse than the alternative model, except for cases where the fraction of stem cells at the
368 steady-state becomes sufficiently big (middle and right column). However, even then the dif-
369 ference between δ_0 and β still needs to be small for the colon model to recover more efficiently.

370

371 *b. Colon model vs. indirect inhibition of stem cell cycling rate* Next, we compare the
372 recovery dynamics of the colon epithelium model with alternative model 3, where the
373 differentiated cell compartment instead of stimulating stem cell differentiation inhibits stem
374 cell cycling. Because the two models have different system parameters (β, δ_0 vs. β_0, δ) we
375 cannot directly compare them pointwise in parameter space like we did before. However,
376 we can still compare the ranges of model defects for the three different perturbations and
377 steady-state stem cell fractions (1%, 10%, and 25%) if we systematically vary the two other
378 free parameters of the models within biologically plausible intervals. In all cases, the defects
379 of the colon epithelium model (Figure 5, Appendix B) and the defects of the alternative
380 model (Figure 7, Appendix B) fall in similar ranges. Hence, there does not seem to be

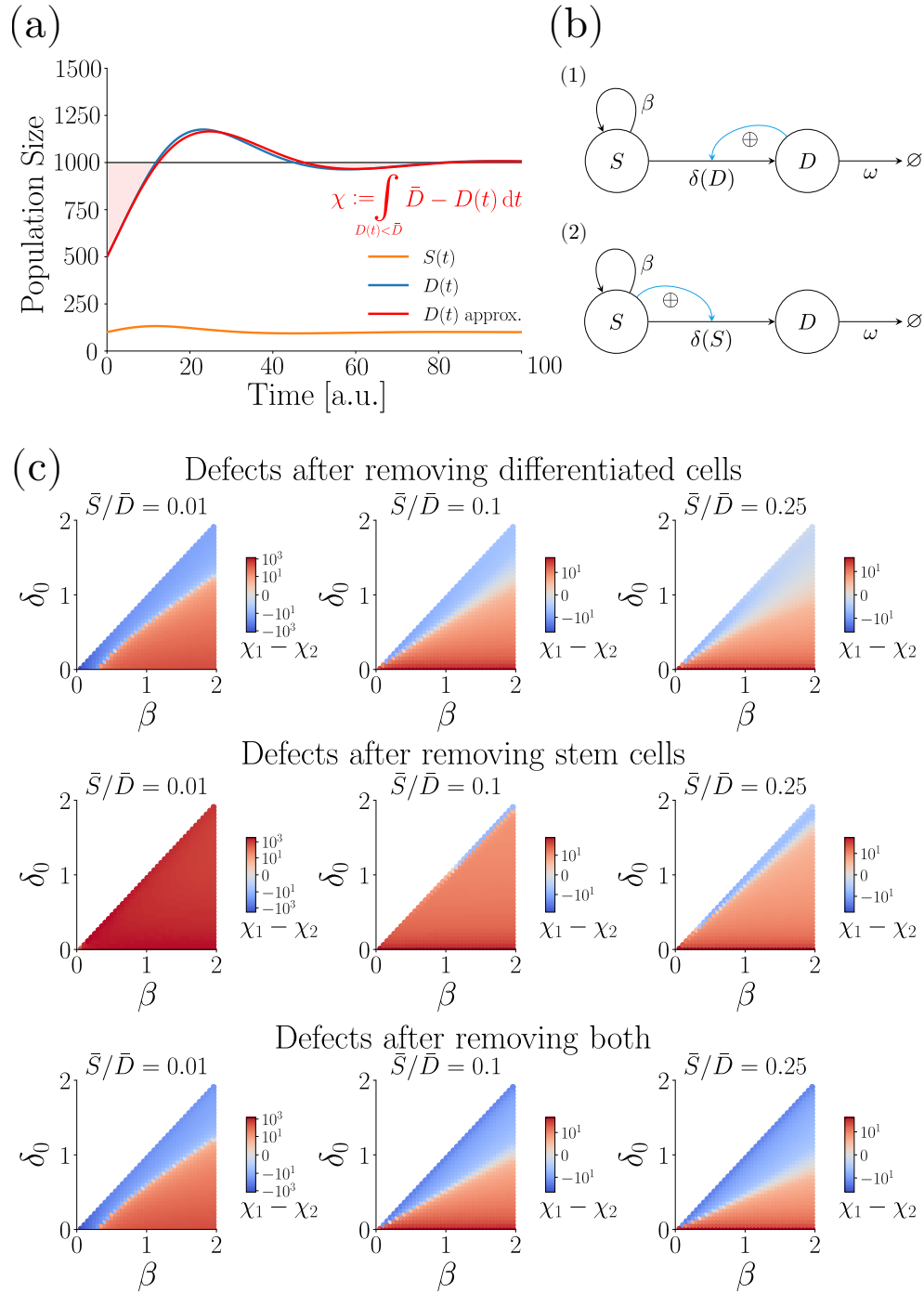


FIG. 3. (a) Illustration of our model comparison: After a perturbation at $t = 0$, the model relaxes to its steady-state (continuous blue and orange lines, depicting differentiated and stem cells, respectively). We use a first-order approximation (continuous red line) in order to not have to rely on costly numerical solutions of the system, and compute the 'defects' χ of the models we want to compare (shaded red area). (b) The two models we compare in this figure. Top: model 1, where stem cell differentiation is stimulated by the differentiated cell compartment; bottom: model 2, where the stem cell compartment stimulates its own differentiation. Note that model 1 is equivalent to our basic colon epithelium model derived earlier. (c) Difference in defects of model 2 and 1 throughout the parameter space. Areas shaded in red depict regions where model 1 shows a bigger defect, i.e. where the colon model recovers less gracefully than the alternative model; blue areas indicate the opposite. Columns represent different cases of stem cell fraction at steady-state (1, 10, and 25% respectively), rows represent the three different kinds of perturbations (removing differentiated cells, removing stem cells, and removing both, respectively).

381 any relevant difference between indirectly regulating stem cell differentiation vs. indirectly
382 regulating stem cell cycling rate with respect to gracefully recovering from perturbations.

383

384 *c. Colon model vs. self-inhibition of stem cell cycling rate* Finally, we compare the recovery
385 dynamics of the colon epithelium model with the behaviour of the remaining model 4, where
386 the stem cell compartment inhibits its own cycling rate. In case of this comparison, we face
387 the same problem of the two models having some different system parameters (β, δ_0 vs. β_0, δ)
388 like in the previous section. We hence follow the same approach as before and compare the
389 ranges of defects occurring in different scenarios. First, notice how in case of the first and
390 third perturbation model 3 performs worse by up to several orders of magnitude if its stem
391 cell differentiation rate δ is small (Figure 8, Appendix B). The only exception to this is
392 the case of a very large steady-state stem cell fraction of 25%. This makes sense, since a
393 small differentiation rate will cause the system to take a longer time to replenish the pool of
394 differentiated cells, even more so if only a small amount of stem cells is present in the first
395 place. In contrast, if differentiated cells are removed from the colon epithelium model, the
396 stem cell differentiation rate will decrease, causing the stem cell compartment to temporarily
397 grow quickly, until the growing differentiated stem cell compartment stimulates differentiation
398 again. This way, the colon epithelium model is able to recover more quickly after removing
399 differentiated tissue. For the remaining case of the second perturbation (removing stem cells),
400 the model defects fall into similar ranges, however the colon epithelium model shows its
401 largest defect in case of a small basal differentiation rate δ_0 , whereas the alternative model
402 performs the worst in case of a very small difference between basal stem cell proliferation
403 rate β and differentiation rate δ . This does make sense, as in this case removing stem cells
404 from model 1 will only cause a very small effective stem cell compartment growth rate of
405 $\beta - \delta_0$, hence the model will take a long time to again completely replenish its stem cell
406 compartment.

407 **C. Dedifferentiation improves recovery from perturbations, however offers an**
408 **additional route of losing homoeostasis**

409 Previously, we have seen that in case of perturbations of the stem cell compartment, in a wide
410 range of parameter values our colon epithelium model does not recover as gracefully as model

411 2, in which stem cell differentiation is stimulated directly by the stem cells themselves (Figure
412 3, medium row). This is caused by the fact that in our colon epithelium model removing
413 stem cells will not alter the rate of stem cell differentiation, since this rate is determined
414 by the number of differentiated cells. Hence, removing stem cells will lead to a significant
415 loss of differentiated cells first, before differentiation rate drops enough for the stem cell
416 compartment to replenish itself, and subsequently replenish the compartment of differentiated
417 cells. This way, the transient behaviour after removing stem cells is characterised by large
418 oscillations in the number of differentiated cells, causing a large model defect.

419

420 We now study how allowing for the dedifferentiation of differentiated cells back into cycling
421 stem cells affects these recovery dynamics of our colon epithelium model (see Panel (a) of
422 Figure 4 for a schematic sketch of the updated colon epithelium model). We again assume
423 for simplicity that the rate of stem cell differentiation is given by a linear function with
424 intercept δ_0 and slope δ_{slope} . We also again assume that the function saturates to a maximum
425 value δ_{max} after some value of D . Hence, we have $\delta(D) = \min\{\delta_0 + \delta_{slope}D, \delta_{max}\}$, where
426 $\delta_0, \delta_{slope}, \delta_{max} > 0$. Next, we also for now assume the same, but horizontally mirrored shape
427 for ϱ , giving $\varrho(S) = \max\{\varrho_0 + \varrho_{slope}S, \varrho_{min}\}$, where $\varrho_0 > 0, \varrho_{slope} < 0, \varrho_{min} \geq 0$.

428

429 For brevity purposes, we present the exact calculations in Appendix C. Briefly, adding a linear
430 dedifferentiation function always causes a faster decay of the oscillations after perturbations.
431 Additionally, we can find a critical value ϱ_0^* , which, when exceeded by ϱ_0 will reduce the
432 frequency of oscillations after perturbations. It is given by

$$\varrho_0^* = (\beta - \delta_0/2)4\omega^2/\beta^2.$$

433 By means of a Taylor expansion around the steady-state, we can also generalise this finding
434 to arbitrary decreasing differentiable functions ϱ .

435

436 Panel (b) of Figure 4 shows some exemplary numerical simulations of our colon epithe-
437 lium model for the case of no dedifferentiation (first column), a linear dedifferentiation
438 with $\varrho_0 = 0.5, \varrho_{slope} = -0.01$ (second column) and a faster linear dedifferentiation with
439 $\varrho_0 = 0.9, \varrho_{slope} = -0.01$. (The other parameters are at their standard values of $\beta = 1$,
440 $\omega = 0.1, \delta_0 = 0.9, \delta_{slope} = -10^{-4}$.) Observe, how the transient period after removing stem

441 cells is characterised by smaller oscillation amplitudes and frequencies dedifferentiation is
442 allowed.

443

444 We also want to study the influence of dedifferentiation on the stability of the non-trivial
445 steady-state of the system. Regardless of the concrete functions δ, ϱ , we find that the non-
446 trivial steady-state needs to satisfy $\beta - \delta(\bar{D}) + (\beta/\omega)\varrho(\bar{S}) = 0$ and $\bar{D} = \beta\bar{S}/\omega$. Hence, a
447 non-trivial steady-state exists, if and only if we can solve

$$\beta - \delta((\beta/\omega)\bar{S}) + (\beta/\omega)\varrho(\bar{S}) = 0, \bar{S} > 0, \quad (4)$$

448 which, importantly, shows that allowing for dedifferentiation enables the system to lose its
449 non-trivial steady-state in another, new way, namely via a sufficient increase of the values of
450 ϱ (see Panel (c) of Figure 4 for an illustration).

451

452 For the case of unbounded growth, it may also be pointed out that under the assumption of
453 a saturating function ϱ converging to ϱ_{min} for sufficiently big values of S , the system will
454 again converge to a stable cell type composition for $t \rightarrow \infty$, given by

$$\lim_{t \rightarrow \infty} \frac{S(t)}{D(t)} = \frac{a + b + w}{2d},$$

455 where $a := \sqrt{4dr + (b + w)^2}$ (see Appendix D for details).

456

IV. DISCUSSION

457 In this work, we have derived and analysed a population dynamics model of the colon epithe-
458 lium, taking into account the stimulating effect of differentiated cells onto the differentiation
459 of stem cells [11–15]. We revealed a number of general properties that hold regardless of the
460 concrete feedback function: In case of any stable steady-state, the number of differentiated
461 cells is not affected by changes in their rate of apoptosis, which is a biologically useful property,
462 since differentiated cells are the cells responsible for carrying out the primary function of a
463 tissue [1, 10] and changes in apoptosis rate may regularly happen locally as a consequence of
464 infections or mechanical wounding [9]. Additionally, we have seen that strong alterations in
465 system parameters are required for the homeostatic steady-state to be destroyed and un-
466 bounded growth to occur – namely the stem cell proliferation rate needs to exceed all possible

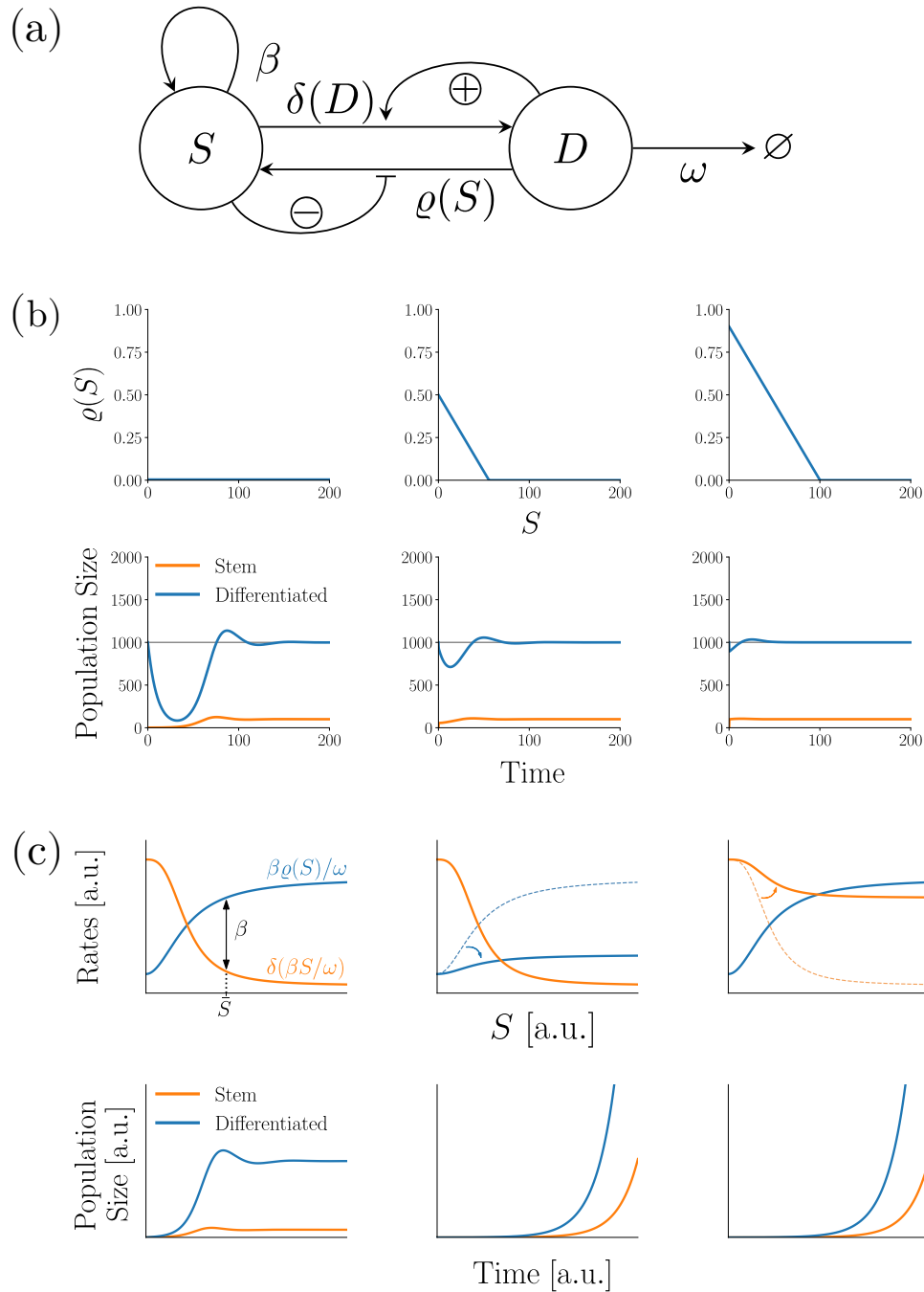


FIG. 4. The colon epithelium model with dedifferentiation and its most important properties. **(a):** Schematic sketch of the model. **(b):** Exemplary numerical simulations of the system with piecewise linear differentiation rate function δ and for different dedifferentiation rate functions ϱ . System parameters are $\beta = 1, \delta_0 = 0.9, \delta_{slope} = 10^{-4}, \omega = 0.1$. Note how adding dedifferentiation, as well as increasing the higher maximum dedifferentiation rate ϱ_0 makes the system recover more gracefully after removing stem cells. **(c):** Adding dedifferentiation opens up a second way the system can lose homoeostatic stability. First column shows the case of homoeostasis. Equilibrium stem cell pool size \bar{S} is given by solving $\beta\varrho(\bar{S})/\omega - \delta(\beta\bar{S}/\omega) = \beta$. Second column: Sufficient decrease of differentiation rate destroys the non-trivial steady-state and unbounded growth occurs. Third column: Sufficient increase of dedifferentiation rate has the same consequence.

467 values of the differentiation rate function. In contrast, any other single alteration, such as a
468 moderate increase in cycling rate or a moderate suppression of dedifferentiation, is not able to
469 cause unbounded growth, but will only change the position of the stable steady-state. This is
470 equivalent to the case of a pre-cancerous lesion, where only a subset of 'canonical' colorectal
471 cancer mutations is yet present and which shows a higher number of cells, but requires further
472 genetic alterations to switch to unbounded growth [37]. Hence, our model recapitulates the
473 observation of colorectal tumorigenesis being a characteristic multi-step process in vivo [38],
474 showcasing the intrinsic resilience of the system towards mutations affecting system properties.

475

476 However, the advantages of an indirect feedback loop onto stem cell differentiation come
477 with the drawback of possible oscillatory behaviour. Depending on the shape of the feedback
478 function, more or – in case of a steeper function – less dampened oscillations around the
479 steady-state may occur. This is reminiscent of e.g. the dampened oscillations observed in
480 the healthy haematopoietic system [39]. In case of feedback functions with a high steepness
481 around the steady-state, these oscillations can even become sustained and undampened. It is
482 a well-known fact that systems with negative feedback loops may exhibit oscillations, even
483 more so in the case of ultrasensitive feedback regulation (for example, see Kholodenko [40]).
484 Hence the oscillatory behaviour of the colon epithelium model comes at no surprise from a
485 mathematical point of view. However, such oscillations in cell numbers do not serve any im-
486 mediately obvious biological purpose and indeed such oscillations may not be at all desirable
487 for upholding tissue homeostasis. This led us to the question whether this way of stabilis-
488 ing the system may offer additional beneficial properties compared to other ways of regulation.

489

490 We thus generalised the derived model to a family of all six imaginable one-looped model
491 topologies. Two of them, namely those where the apoptosis rate of differentiated cells is
492 controlled, cannot exhibit homeostasis, showing that a mechanism controlling cycling stem
493 cells is required for stability, be it in the form of controlling their proliferation rate, their
494 differentiation rate, or potentially both. We have shown that if all of these control mechanisms
495 originate exclusively from the differentiated cell compartment, the steady-state size of the
496 differentiated cell compartment will still not be affected by changes in apoptosis rate. In
497 contrast, if the stem cell compartment is exclusively regulated by itself, the steady-state
498 density of stem cells, but not of differentiated cells will be unaffected by changes in apoptosis

499 rate. Because the differentiated cells are responsible for carrying out the designated function
500 of a tissue [1], keeping their density as constant as possible is biologically desirable and
501 thus grants systems with indirectly regulated stem cell compartments an advantage – even
502 more so in tissues like the intestinal and colon epithelium which are constantly exposed to
503 mechanical, chemical and biological insults [9].

504

505 We also revealed pronounced differences of the four stable model topologies regarding their
506 ability to quickly return to their steady-state after external perturbations. We have shown
507 the existence of ample regions in parameter space where the colon epithelium model recovers
508 more gracefully from removing differentiated tissue compared to an alternative model,
509 where stem cells stimulate their own differentiation. This makes sense because removing
510 stem cells from the colon epithelium model cells will cause stem cells to differentiate more
511 slowly. Hence the stem cell compartment can 'overshoot', until the growing compartment of
512 differentiated cells forces more and more stem cells to differentiate. Thus, the differentiated
513 cell compartment can be replenished quickly. However in case of removing stem cells, the
514 colon model very often performed significantly worse since removing stem cells will not
515 affect stem cell cycling and stem cell differentiation rates in the colon epithelium model. If,
516 however, the differentiated cell compartment does not stimulate stem cell differentiation,
517 but instead inhibits stem cell cycling, the recovery dynamics of the system do not seem
518 to significantly change. Finally, if, in contrast, stem cells inhibit their own proliferation,
519 the system generally performs worse compared to the colon epithelium model, regardless
520 of which perturbation is applied. All in all, the colon epithelium model seems to generally
521 show a significantly better or at least similar recovery behaviour compared to other model
522 topologies except for the case of removing stem cells.

523

524 The inefficient relaxation dynamics of our colon model in case of stem cell removal prompted
525 us to study the behaviour of our model if we additionally allow for dedifferentiation of
526 differentiated cells back into cycling stem cells. We have shown both analytically and by
527 exemplary numerical simulations how this enables the model to recover more gracefully from
528 perturbations, especially those reducing the number of stem cells. Such a perturbations for
529 instance represents the case of radiation-induced stem cell death [41]. However, adding the
530 possibility of dedifferentiation to the system can also cause the destruction of the non-trivial

531 steady-state. This is biologically interesting, because it suggests that a sufficient increase in
532 dedifferentiation rates may offer an alternative route of escaping homeostatic control and
533 entering a regime of unbounded, malignant growth of the tissue. Recent experimental data
534 seems to indeed confirm this possibility of tumours arising from the differentiated intestinal
535 epithelium as a consequence of inactivation of the differentiation-promoting transcription
536 factor *SMAD4* [42]. Interestingly, mutations in *SMAD4* do indeed occur rather often in
537 colorectal cancers [43, 44], suggesting that increased dedifferentiation might regularly con-
538 tribute to colorectal tumorigenesis. Experimental data by Nakano *et al.* [45] points into the
539 same direction, showing how dedifferentiation processes increase stemness in colorectal cancer.

540

541 Obviously, the introduction of the dedifferentiation term affects the steady-state position of
542 the system, and one may easily verify (by writing Equation 4 in terms of \bar{D}) that its addition
543 interferes with the invariance of the steady-state size of the differentiated cell compartment
544 to changes in apoptosis rate. However, if the dedifferentiation rate around the steady-state
545 is small and only becomes noticeable if a sizeable fraction of stem cells is removed (which
546 seems to be suggested by the literature, see Tata *et al.* [4] and Beumer and Clevers [8]), then
547 around the steady-state the dedifferentiation term becomes neglectable and the number of
548 differentiated cells at steady-state stays invariant to changes in apoptosis rate.

549

550 We have also revealed that in case of a tissue which has switched to exhibiting unbounded
551 growth, after a period of transient behaviour we will – under the biological reasonable
552 assumption of saturating feedback functions – observe the convergence to a stable ratio of
553 cycling stem cells and noncycling differentiated cells. This happens both in case of the colon
554 epithelium model, as well as in case of all other studied model topologies, and is not affected
555 by whether dedifferentiation of differentiated cells is possible or not. From a biological
556 point of view, this is interesting because it directly relates to the topic of intratumoural
557 heterogeneity [46–48], and suggest that after acquiring mutations and switching to unbounded
558 growth the colon epithelium can still be expected to recapitulate known cellular hierarchies
559 and differentiation gradients. In case of breast cancer [49] and cancers of the haematopoietic
560 system [50] this has already been observed experimentally.

561

562 An interesting avenue for future research lies in the examination of healthy and tumoural

563 intestinal epithelial tissue on the single-cell level in order to answer the question, whether
564 we are indeed able to identify similar cellular subpopulation and differentiation gradients
565 in both of them. Very recent research seems to in fact suggest exactly this [51]. If this
566 holds, tracking the numbers of different cell types over time during development and after
567 perturbations would yield valuable data for validating and more accurately parametrising the
568 model derived in this work. Additionally, comparing the quantitative behaviour of tissues in
569 different stages of tumorigenesis could inform us at which of these stages which properties
570 of the system are changed in which way compared to healthy tissue, and thus increase our
571 mechanistic insight into the dynamics of tumour development. Such an increased mechanistic
572 insight, in turn, might ultimately help to contribute to the development of novel approaches
573 to limiting tumoural growth *in vivo*.

574

ACKNOWLEDGMENTS

575 We thank Christine Sers and Markus Morkel for fruitful discussions and helpful comments
576 during an early stage of this project and DFG for funding (RTG2424, CompCancer).

577

AUTHOR DECLARATIONS

578

A. Conflicts of interest

579 All authors declare no conflict of interest.

580

B. Code availability

581 All source code for the reproduction of the numerical analyses is available in the following
582 github repository: <https://github.com/Matthias-M-Fischer/Epithelium>

583

C. Author contributions

584 All authors conceived of the presented ideas; M.M.F. carried out model derivations and
585 analyses with help from N.B. and input from H.H; M.M.F. produced the initial version of
586 the manuscript with help from N.B; H.H. and N.B. contributed to the final version of the

587 manuscript; N.B. supervised the project. All authors have read and approve of the final
588 version of this manuscript.

-
- 589 [1] I. L. Weissman, Stem cells: units of development, units of regeneration, and units in evolution,
590 *Cell* **100**, 157 (2000).
- 591 [2] Y. Liu and Y.-G. Chen, Intestinal epithelial plasticity and regeneration via cell dedifferentiation,
592 *Cell Regeneration* **9**, 1 (2020).
- 593 [3] Y. Liu, X. Xiong, and Y.-G. Chen, Dedifferentiation: the return road to repair the intestinal
594 epithelium, *Cell Regeneration* **9**, 1 (2020).
- 595 [4] P. R. Tata, H. Mou, A. Pardo-Saganta, R. Zhao, M. Prabhu, B. M. Law, V. Vinarsky, J. L.
596 Cho, S. Breton, A. Sahay, *et al.*, Dedifferentiation of committed epithelial cells into stem cells
597 in vivo, *Nature* **503**, 218 (2013).
- 598 [5] J. V. Bonventre, Dedifferentiation and proliferation of surviving epithelial cells in acute renal
599 failure, *Journal of the American Society of Nephrology* **14**, S55 (2003).
- 600 [6] B. Biteau, C. E. Hochmuth, and H. Jasper, Maintaining tissue homeostasis: dynamic control
601 of somatic stem cell activity, *Cell stem cell* **9**, 402 (2011).
- 602 [7] F. M. Watt and B. L. Hogan, Out of eden: stem cells and their niches, *Science* **287**, 1427
603 (2000).
- 604 [8] J. Beumer and H. Clevers, Regulation and plasticity of intestinal stem cells during homeostasis
605 and regeneration, *Development* **143**, 3639 (2016).
- 606 [9] H. Gehart and H. Clevers, Tales from the crypt: new insights into intestinal stem cells, *Nature*
607 *Reviews Gastroenterology & Hepatology* **16**, 19 (2019).
- 608 [10] L. G. Van Der Flier and H. Clevers, Stem cells, self-renewal, and differentiation in the intestinal
609 epithelium, *Annual review of physiology* **71**, 241 (2009).
- 610 [11] G. R. Van Den Brink, S. A. Bleuming, J. C. Hardwick, B. L. Schepman, G. J. Offerhaus, J. J.
611 Keller, C. Nielsen, W. Gaffield, S. J. Van Deventer, D. J. Roberts, *et al.*, Indian hedgehog is
612 an antagonist of wnt signaling in colonic epithelial cell differentiation, *Nature genetics* **36**, 277
613 (2004).
- 614 [12] B. B. Madison, K. Braunstein, E. Kuizon, K. Portman, X. T. Qiao, and D. L. Gumucio,
615 Epithelial hedgehog signals pattern the intestinal crypt-villus axis, *Development* **132**, 279

- 616 (2005).
- 617 [13] L. E. Batts, D. B. Polk, R. N. Dubois, and H. Kulesa, Bmp signaling is required for intestinal
618 growth and morphogenesis, *Developmental dynamics: an official publication of the American*
619 *Association of Anatomists* **235**, 1563 (2006).
- 620 [14] W. A. Van Dop, J. Heijmans, N. V. Büller, S. A. Snoek, S. L. Rosekrans, E. A. Wassenberg,
621 M. A. van den Bergh Weerman, B. Lanske, A. R. Clarke, D. J. Winton, *et al.*, Loss of
622 indian hedgehog activates multiple aspects of a wound healing response in the mouse intestine,
623 *Gastroenterology* **139**, 1665 (2010).
- 624 [15] N. V. Büller, S. L. Rosekrans, J. Westerlund, and G. R. van den Brink, Hedgehog signaling
625 and maintenance of homeostasis in the intestinal epithelium, *Physiology* **27**, 148 (2012).
- 626 [16] I. A. Rodriguez-Brenes, N. L. Komarova, and D. Wodarz, Evolutionary dynamics of feedback
627 escape and the development of stem-cell–driven cancers, *Proceedings of the National Academy*
628 *of Sciences* **108**, 18983 (2011).
- 629 [17] I. A. Rodriguez-Brenes, D. Wodarz, and N. L. Komarova, Stem cell control, oscillations, and
630 tissue regeneration in spatial and non-spatial models, *Frontiers in oncology* **3**, 82 (2013).
- 631 [18] Z. Sun and N. L. Komarova, Stochastic control of proliferation and differentiation in stem cell
632 dynamics, *Journal of Mathematical Biology* **71**, 883 (2015).
- 633 [19] D. Wodarz, Effect of cellular de-differentiation on the dynamics and evolution of tissue and
634 tumor cells in mathematical models with feedback regulation, *Journal of theoretical biology*
635 **448**, 86 (2018).
- 636 [20] I. Roeder and M. Loeffler, A novel dynamic model of hematopoietic stem cell organization
637 based on the concept of within-tissue plasticity, *Experimental hematology* **30**, 853 (2002).
- 638 [21] I. Glauche, M. Cross, M. Loeffler, and I. Roeder, Lineage specification of hematopoietic stem
639 cells: mathematical modeling and biological implications, *Stem cells* **25**, 1791 (2007).
- 640 [22] I. Glauche, M. Horn, and I. Roeder, Leukaemia stem cells: hit or miss?, *British journal of*
641 *cancer* **96**, 677 (2007).
- 642 [23] F. Michor *et al.*, Mathematical models of cancer stem cells, *Journal of Clinical Oncology* **26**,
643 2854 (2008).
- 644 [24] A. Marciniak-Czochra, T. Stiehl, A. D. Ho, W. Jäger, and W. Wagner, Modeling of asymmetric
645 cell division in hematopoietic stem cells—regulation of self-renewal is essential for efficient
646 repopulation, *Stem cells and development* **18**, 377 (2009).

- 647 [25] A. D. Lander, K. K. Gokoffski, F. Y. Wan, Q. Nie, and A. L. Calof, Cell lineages and the logic
648 of proliferative control, *PLoS Biol* **7**, e1000015 (2009).
- 649 [26] W.-C. Lo, C.-S. Chou, K. K. Gokoffski, F. Y.-M. Wan, A. D. Lander, A. L. Calof, and Q. Nie,
650 Feedback regulation in multistage cell lineages, *Mathematical biosciences and engineering*:
651 *MBE* **6**, 59 (2009).
- 652 [27] H. Enderling, M. A. Chaplain, A. R. Anderson, and J. S. Vaidya, A mathematical model of
653 breast cancer development, local treatment and recurrence, *Journal of Theoretical Biology*
654 **246**, 245 (2007).
- 655 [28] M. D. Johnston, C. M. Edwards, W. F. Bodmer, P. K. Maini, and S. J. Chapman, Mathematical
656 modeling of cell population dynamics in the colonic crypt and in colorectal cancer, *Proceedings*
657 *of the National Academy of Sciences* **104**, 4008 (2007).
- 658 [29] P.-F. Verhulst, Notice sur la loi que la population suit dans son accroissement, *Corresp. Math.*
659 *Phys.* **10**, 113 (1838).
- 660 [30] A. J. Lotka, Analytical note on certain rhythmic relations in organic systems, *Proceedings of*
661 *the National Academy of Sciences* **6**, 410 (1920).
- 662 [31] V. Volterra, *Fluctuations in the abundance of a species considered mathematically* 1 (1926).
- 663 [32] M. Peschel and W. Mende, *The predator-prey model: do we live in a Volterra world?* (Springer,
664 1986).
- 665 [33] S. Legewie, B. Schoeberl, N. Blüthgen, and H. Herzel, Competing docking interactions can
666 bring about bistability in the mapk cascade, *Biophysical journal* **93**, 2279 (2007).
- 667 [34] G. Van Rossum and F. L. Drake Jr, *Python tutorial* (Centrum voor Wiskunde en Informatica
668 Amsterdam, The Netherlands, 1995).
- 669 [35] G. Jetschke, *Mathematik der Selbstorganisation* (Springer, 1989).
- 670 [36] S. H. Strogatz, *Nonlinear dynamics and chaos with student solutions manual: With applications*
671 *to physics, biology, chemistry, and engineering* (CRC press, 2018).
- 672 [37] T. Muto, H. Bussey, and B. Morson, The evolution of cancer of the colon and rectum, *Cancer*
673 **36**, 2251 (1975).
- 674 [38] E. R. Fearon and B. Vogelstein, A genetic model for colorectal tumorigenesis, *cell* **61**, 759
675 (1990).
- 676 [39] A. Marciniak-Czochra and T. Stiehl, Mathematical models of hematopoietic reconstitution
677 after stem cell transplantation, in *Model Based Parameter Estimation* (Springer, 2013) pp.

678 191–206.

679 [40] B. N. Kholodenko, Negative feedback and ultrasensitivity can bring about oscillations in the
680 mitogen-activated protein kinase cascades, *European journal of biochemistry* **267**, 1583 (2000).

681 [41] C. S. Potten and H. Grant, The relationship between ionizing radiation-induced apoptosis and
682 stem cells in the small and large intestine, *British journal of cancer* **78**, 993 (1998).

683 [42] A. O. Perekatt, P. P. Shah, S. Cheung, N. Jariwala, A. Wu, V. Gandhi, N. Kumar, Q. Feng,
684 N. Patel, L. Chen, *et al.*, Smad4 suppresses wnt-driven dedifferentiation and oncogenesis in
685 the differentiated gut epithelium, *Cancer research* **78**, 4878 (2018).

686 [43] M. Miyaki, T. Iijima, M. Konishi, K. Sakai, A. Ishii, M. Yasuno, T. Hishima, M. Koike,
687 N. Shitara, T. Iwama, *et al.*, Higher frequency of smad4 gene mutation in human colorectal
688 cancer with distant metastasis, *Oncogene* **18**, 3098 (1999).

689 [44] N. I. Fleming, R. N. Jorissen, D. Mouradov, M. Christie, A. Sakthianandeswaren, M. Palmieri,
690 F. Day, S. Li, C. Tsui, L. Lipton, *et al.*, Smad2, smad3 and smad4 mutations in colorectal
691 cancer, *Cancer research* **73**, 725 (2013).

692 [45] M. Nakano, Y. Kikushige, K. Miyawaki, Y. Kunisaki, S. Mizuno, K. Takenaka, S. Tamura,
693 Y. Okumura, M. Ito, H. Ariyama, *et al.*, Dedifferentiation process driven by tgf-beta signaling
694 enhances stem cell properties in human colorectal cancer, *Oncogene* **38**, 780 (2019).

695 [46] M. Brattain, A. Levine, S. Chakrabarty, L. Yeoman, J. Willson, and B. Long, Heterogeneity of
696 human colon carcinoma, *Cancer and Metastasis Reviews* **3**, 177 (1984).

697 [47] D. Buob, H. Fauvel, M.-P. Buisine, S. Truant, C. Mariette, N. Porchet, A. Wacrenier, M.-C.
698 Copin, and E. Leteurtre, The complex intratumoral heterogeneity of colon cancer highlighted
699 by laser microdissection, *Digestive diseases and sciences* **57**, 1271 (2012).

700 [48] C. K. Sievers, A. A. Leystra, L. Clipson, W. F. Dove, and R. B. Halberg, Understanding
701 intratumoral heterogeneity: lessons from the analysis of at-risk tissue and premalignant lesions
702 in the colon, *Cancer prevention research* **9**, 638 (2016).

703 [49] M. Al-Hajj, M. S. Wicha, A. Benito-Hernandez, S. J. Morrison, and M. F. Clarke, Prospective
704 identification of tumorigenic breast cancer cells, *Proceedings of the National Academy of*
705 *Sciences* **100**, 3983 (2003).

706 [50] D. Bonnet and J. E. Dick, Human acute myeloid leukemia is organized as a hierarchy that
707 originates from a primitive hematopoietic cell, *Nature medicine* **3**, 730 (1997).

708 [51] W. R. Becker, S. A. Nevins, D. C. Chen, R. Chiu, A. Horning, R. Laquindanum, M. Mills,
709 H. Chaib, U. Ladabaum, T. Longacre, *et al.*, Single-cell analyses reveal a continuum of cell
710 state and composition changes in the malignant transformation of polyps to colorectal cancer,
711 bioRxiv (2021).

712

Appendix A: Model dynamics after perturbations

713 Let $(\Delta S(0), \Delta D(0))$ denote a perturbation away from the steady-state (\bar{S}, \bar{D}) of a system at
 714 $t = 0$. Let $\vec{q}(t) = [\Delta S(t), \Delta D(t)]^T$ denote the dynamics of the displacement after the perturba-
 715 tion. We can approximate to first order $d\vec{q}(t)/dt \approx \mathbf{J}_{eq}\vec{q}(t)$, where \mathbf{J}_{eq} denotes the Jacobian of
 716 the system at the steady-state. This linear system is then solved by $\vec{q}(t) = c_1 e^{\lambda_1 t} \vec{u}_1 + c_2 e^{\lambda_2 t} \vec{u}_2$,
 717 where $\lambda_{1,2}$ denote the eigenvalues of \mathbf{J}_{eq} , $\vec{u}_{1,2}$ denote their corresponding eigenvectors, and
 718 $c_{1,2} \in \mathbb{C}$ are to be chosen to satisfy the initial condition $\vec{q}(0) = [\bar{S} + \Delta S(0), \bar{D} + \Delta D(0)]^T$.

719

720 Because model 1 may show oscillations during its relaxation, an analytical calculation of
 721 its defects is theoretically possible, but leads to expressions too complicated to handle and
 722 meaningfully interpret. For this reason, we instead only derive the approximative relaxation
 723 dynamics of the model for the three perturbations and will calculate the corresponding model
 724 defects numerically. We get:

$$\Delta D_1(t) = \begin{cases} \Delta D(0) \frac{\cosh(rt) - (d/r) \sinh(rt)}{e^{dt}} & \text{First perturbation} \\ \Delta S(0) \beta \frac{\sinh(rt)}{r e^{dt}} & \text{Second perturbation} \\ \Delta D(0) \frac{\cosh(rt) - (d/r) \sinh(rt)}{e^{dt}} + \Delta S(0) \beta \frac{\sinh(rt)}{r e^{dt}} & \text{Third perturbation,} \end{cases}$$

725 where $d := \delta_0 \omega / (2\beta)$, and $r := \sqrt{-4\beta^3 \omega + 4\beta^2 \delta_0 \omega + \delta_0^2 \omega^2} / (2\beta)$.

726

727 Next, we calculate the defects χ_2 of model 2 for the three perturbations. For the case of the
 728 first perturbation, the defect can be directly obtained by solving the system analytically for
 729 $S(0) = \bar{S}, D(0) = 0$ and calculating the integral. The other two defects are obtained by using
 730 the first-order approximation of the dynamics derived earlier and analytically calculating
 731 their integrals after choosing the respective initial conditions. We get:

$$\chi_2 = \begin{cases} \Delta D(0) \frac{1}{\omega} & \text{First perturbation} \\ \Delta S(0) \frac{2\beta - \delta_0}{\beta - \delta_0 - \omega} (1/(\delta_0 - \beta) + 1/\omega) & \text{Second perturbation} \\ \Delta D(0) \frac{1}{\omega} + \Delta S(0) \frac{2\beta - \delta_0}{\beta - \delta_0 - \omega} (1/(\delta_0 - \beta) + 1/\omega) & \text{Third perturbation.} \end{cases}$$

732 For model 3, we again only derive the relaxation dynamics after the three perturbations, and
 733 will examine them numerically. They are given by:

$$\Delta D_3(t) = \begin{cases} \Delta D(0) \frac{\cosh(rt) - (d/r) \sinh(rt)}{e^{dt}} & \text{First perturbation} \\ \Delta S(0) \frac{\delta \sinh(rt)}{r e^{dt}} & \text{Second perturbation} \\ \Delta D(0) \frac{\cosh(rt) - (d/r) \sinh(rt)}{e^{dt}} + \Delta S(0) \frac{\delta \sinh(rt)}{r e^{dt}} & \text{Third perturbation,} \end{cases}$$

⁷³⁴ where $d := \omega/2$, and $r := \sqrt{\omega(-4\beta_0 + 4\delta + \omega)}/2$.

⁷³⁵

⁷³⁶ For model 4, we can analytically calculate the defects after the three perturbations. They

⁷³⁷ are:

$$\chi_4 = \begin{cases} \Delta D(0) \frac{1}{\omega} & \text{First perturbation} \\ \Delta S(0) \frac{\delta}{(\beta_0 - \delta)\omega} & \text{Second perturbation} \\ \Delta D(0) \frac{1}{\omega} + \Delta S(0) \frac{\delta}{(\beta_0 - \delta)\omega} & \text{Third perturbation.} \end{cases}$$

738

Appendix B: Model dynamics after perturbations

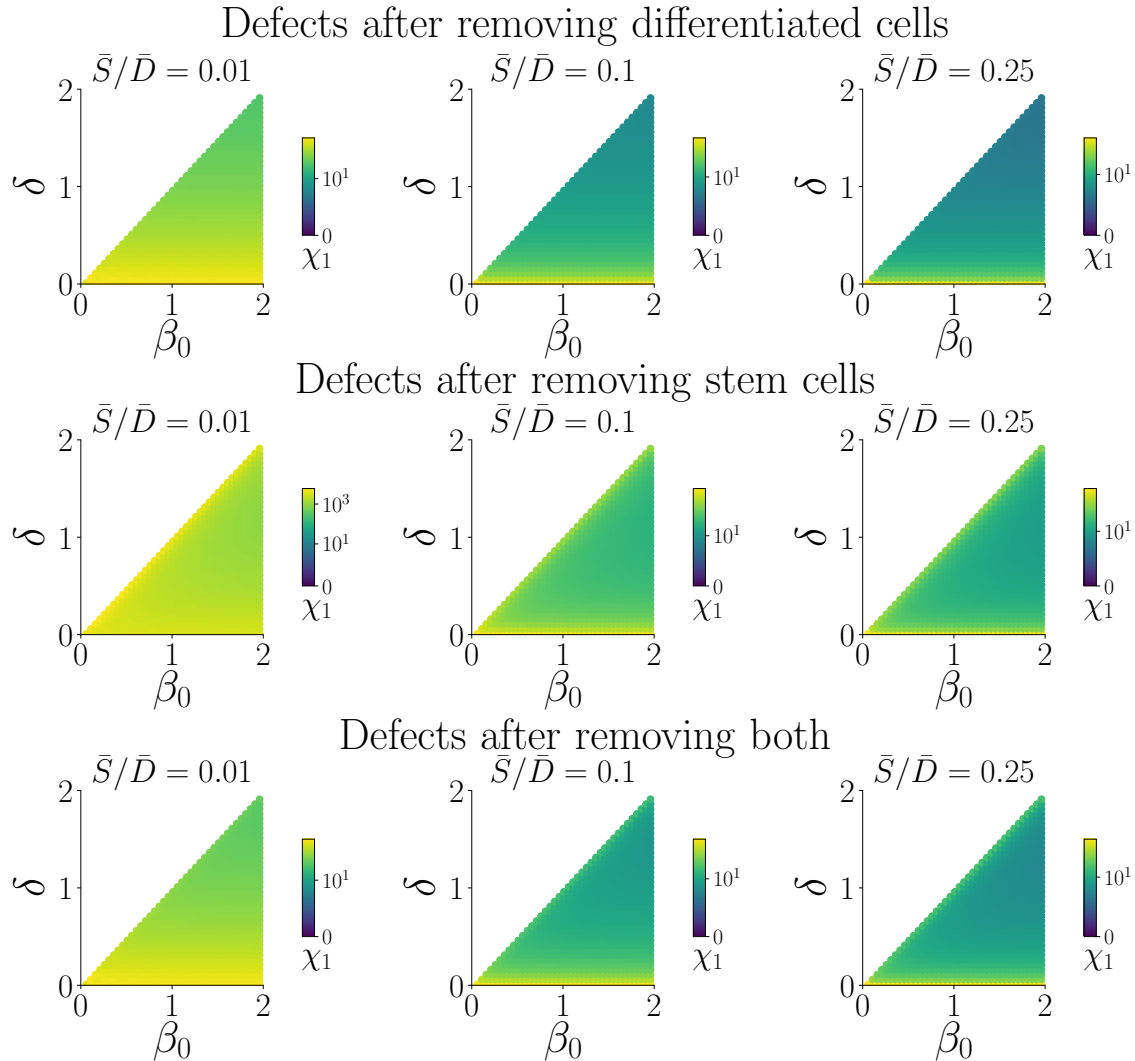


FIG. 5. The model defects χ_1 of model 1, the colon epithelium model, throughout its parameter space. Defects are given in multiples of initial perturbation size. Columns represent three different scenarios with different steady-state stem cell fractions of 1%, 10%, and 25%, respectively.

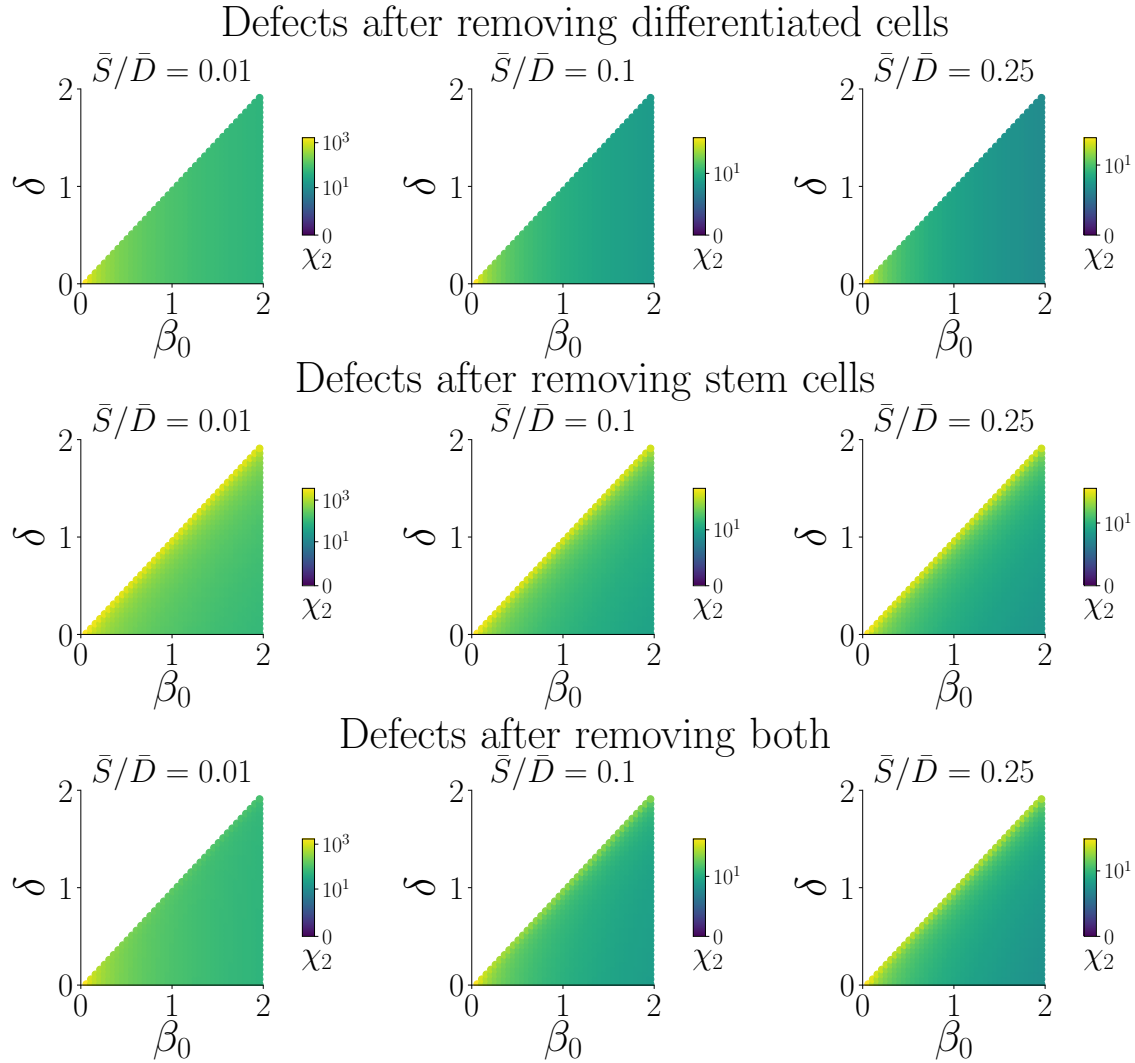


FIG. 6. The model defects χ_2 of model 1, the colon epithelium model, throughout its parameter space. Defects are given in multiples of initial perturbation size. Columns represent three different scenarios with different steady-state stem cell fractions of 1%, 10%, and 25%, respectively.

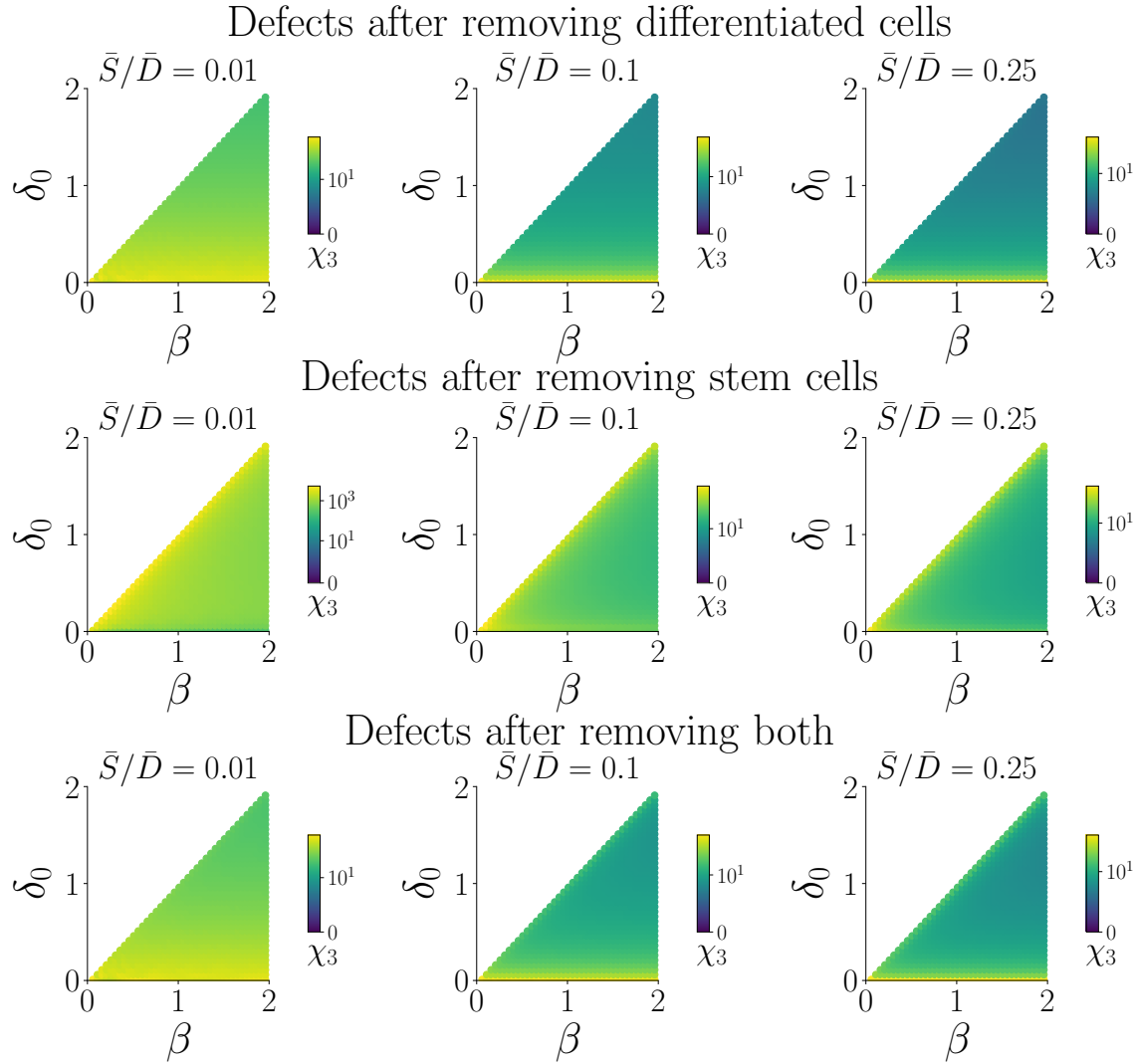


FIG. 7. The model defects χ_3 of model 3, where stem cell cycling rate is controlled by the number of differentiated cells, throughout its parameter space. Defects are given in multiples of initial perturbation size. Columns represent three different scenarios with different steady-state stem cell fractions of 1%, 10%, and 25%, respectively.

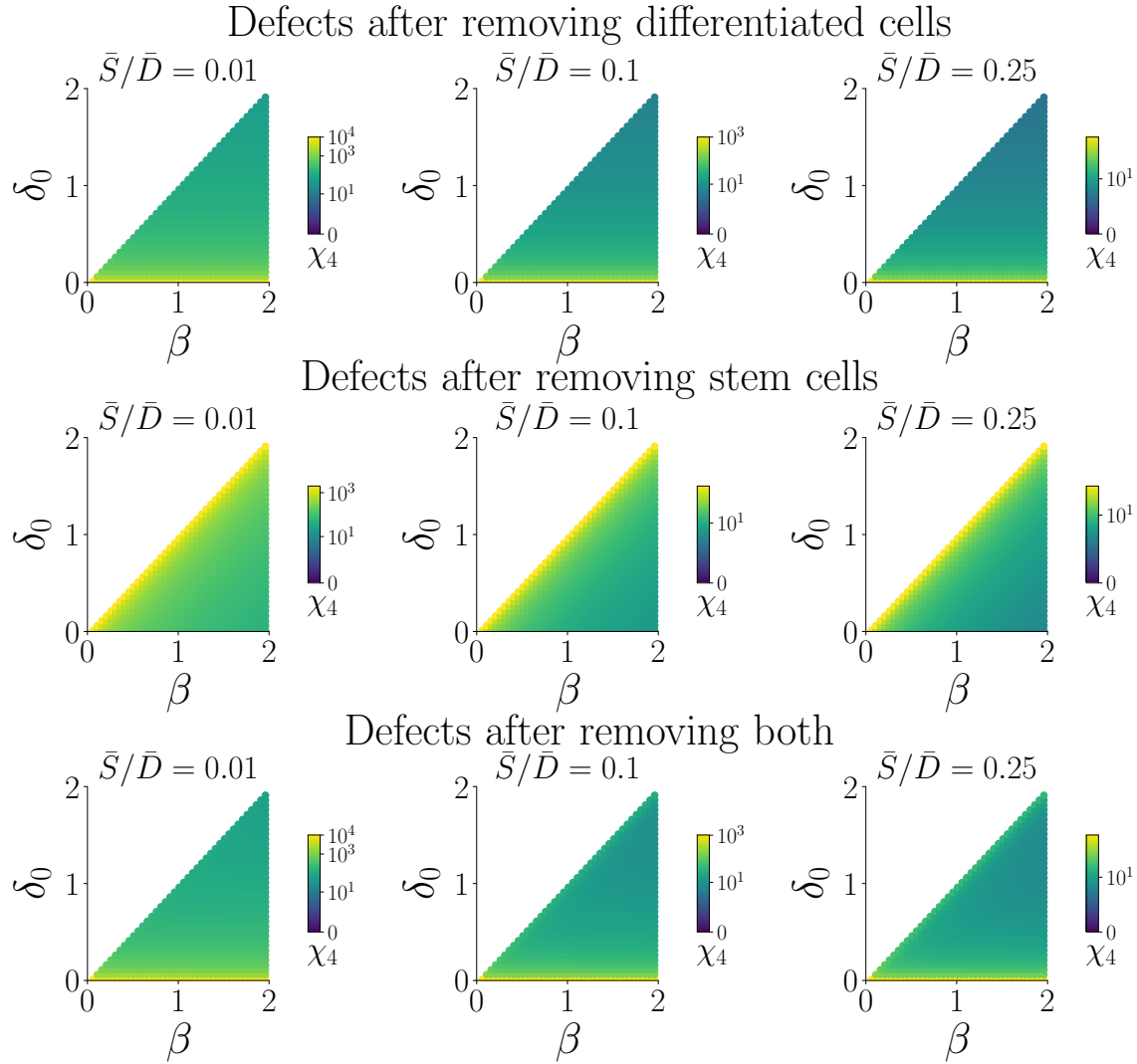


FIG. 8. The model defects χ_4 of model 4, where the stem cell compartment inhibits its own cycling rate, throughout its parameter space. Defects are given in multiples of initial perturbation size. Columns represent three different scenarios with different steady-state stem cell fractions of 1%, 10%, and 25%, respectively.

739

Appendix C: Dedifferentiation can limit oscillatory behaviour

740 The modified model permits exactly one non-trivial steady-state at

$$\bar{S} = -\frac{(\beta - \delta_0)\omega + \varrho_0\beta}{\beta(\varrho_{slope} - \delta_{slope})}; \bar{D} = \beta\bar{S}/\omega,$$

741 and its Jacobian at this steady-state is given by

$$\mathbf{J}_{eq} = \begin{pmatrix} -\frac{\varrho_0\beta}{\omega} & -\frac{(\beta - \delta_0)\omega}{\beta} \\ \beta + \frac{\varrho_0\beta}{\omega} & \frac{(\beta - \delta_0)\omega}{\beta} - \omega. \end{pmatrix}$$

742 This matrix has eigenvalues

$$\lambda_{1,2} = \frac{-\beta^2\varrho_0 - \delta_0\omega^2 \pm \sqrt{(\beta^2 - \varrho_0 + \delta_0\omega^2)^2 - 4(\beta^3\varrho_0\omega^2 + \beta^3\omega^3 - \beta^2\delta_0\omega^3)}}{2\beta\omega}$$

743 If oscillations occur, we have complex eigenvalues, which we can split into a real and an
744 imaginary part as follows:

$$\Re(\lambda_{1,2}) = -\frac{\beta\varrho_0}{2\omega} - \frac{\delta_0\omega}{2\beta}; \Im(\lambda_{1,2}) = \frac{\sqrt{(-\beta^2 - \varrho_0 + \delta_0\omega^2)^2 + 4(\beta^3\varrho_0\omega^2 + \beta^3\omega^3 - \beta^2\delta_0\omega^3)}}{2\beta\omega}.$$

745 For the colon epithelium model without differentiation the real part of the complex eigen-
746 values of the Jacobian at steady-state was given by $-\delta_0\omega/(2\beta)$. Accordingly, additionally
747 allowing for dedifferentiation reduces the real part by $\beta\varrho_0/(2\omega) > 0$, hence always causing a
748 faster decay of the oscillations after perturbations.

749

750 For the model without dedifferentiation we had an imaginary part of the eigenvalues of
751 $\sqrt{4\beta^3\omega - 4\beta^2\delta_0\omega - \delta_0^2\omega^2}/(2\beta)$. Hence, adding the dedifferentiation to the model changes the
752 radicand of the imaginary part of the eigenvalues by

$$\Delta = \beta\varrho_0 - \frac{\beta^2\varrho^2}{4\omega^2} - \frac{\varrho_0\delta_0}{2}.$$

753 Thus, we can find a critical value ϱ_0^* , which, when exceeded by ϱ_0 will reduce the frequency
754 of oscillations after perturbations. It is given by

$$\varrho_0^* = (\beta - \delta_0/2)4\omega^2/\beta^2.$$

755 In other words, adding a linear dedifferentiation function will speed up the amplitude
756 decay of the oscillations after perturbations and can also, in case of a sufficiently big basal
757 dedifferentiation rate, decrease the frequency of these oscillations.

758

759 We can generalise this finding to arbitrary decreasing differentiable functions ϱ . To this end, we
760 construct a Taylor expansion of ϱ around the steady-state of the form $\varrho(D) \approx a + bD + \mathcal{O}(D^2)$
761 with $a, b \in \mathbb{R}$. This way, in a sufficiently small neighbourhood around the steady-state,
762 the system behaves as if ϱ was linear; and because ϱ by definition is always positive and
763 monotonously decreasing, clearly $b < 0$ and accordingly $a > 0$. Hence, the argument for
764 linear functions ϱ we made previously also applies here when we simply replace ϱ_0 with a .

765

766 **Appendix D: Convergence of the colon epithelium model with dedifferentiation to a**
767 **stable cell type ratio**

768 For sufficiently high population sizes, the dynamics of the system are governed by the set of
769 linear differential equations

$$\begin{aligned}\frac{dS(t)}{dt} &= \beta S(t) - \delta_{max} S(t) + \varrho_{min} D(t) \\ \frac{dD(t)}{dt} &= \delta_{max} S(t) - \varrho_{min} D(t) - \omega D(t).\end{aligned}$$

770 For convenience, we define $b := \beta - \delta_{max}$, $w := \omega + \varrho_{min}$, $r := \varrho_{min}$, $d := \delta_{max}$, giving

$$\begin{aligned}\frac{dS(t)}{dt} &= bS(t) + rD(t) \\ \frac{dD(t)}{dt} &= dS(t) - wD(t).\end{aligned}$$

771 This system has the general solution

$$\begin{aligned}S(t) &= \frac{(a - b - w)S_0 - 2rD_0 + ((a + b + w)S_0 + 2rD_0)e^{at}}{2ae^{\frac{a-b+w}{2}t}} \\ D(t) &= \frac{-2dS_0 + (a + b + w)D_0 + (2dS_0 + (a - b - w)D_0)e^{at}}{2ae^{\frac{a-b+w}{2}t}},\end{aligned}$$

772 where $a := \sqrt{4dr + (b + w)^2}$. Taking the limit yields

$$\lim_{t \rightarrow \infty} \frac{S(t)}{D(t)} = \frac{a + b + w}{2d}.$$